Article

Origin of Strong Chiroptical Activities in Films of Nonafluorenes with a Varying Extent of Pendant Chirality

Yanhou Geng, Anita Trajkovska, Sean W. Culligan, Jane J. Ou, H. M. Philip Chen, Dimitris Katsis, and Shaw H. Chen

J. Am. Chem. Soc., **2003**, 125 (46), 14032-14038• DOI: 10.1021/ja037733e • Publication Date (Web): 25 October 2003

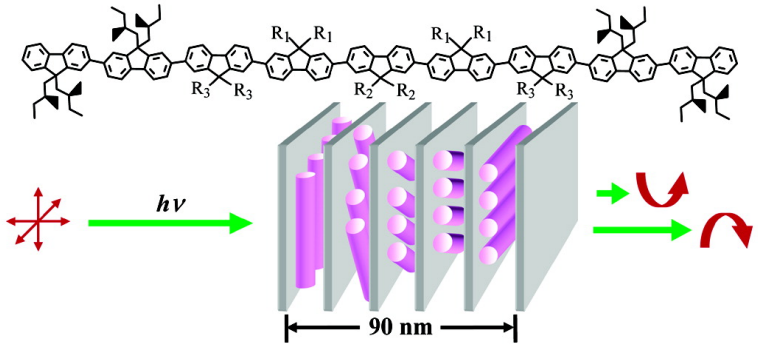

More About This Article

Additional resources and features associated with this article are available within the HTML version:

- Supporting Information
- Links to the 15 articles that cite this article, as of the time of this article download
- Access to high resolution figures
- Links to articles and content related to this article
- Copyright permission to reproduce figures and/or text from this article

View the Full Text HTML

J|A|C|S
ARTICLES
Published on Web 10/25/2003

Origin of Strong Chiroptical Activities in Films of Nonafluorenes with a Varying Extent of Pendant Chirality

Yanhou Geng,[†] Anita Trajkovska,[†] Sean W. Culligan,[†] Jane J. Ou,[†] H. M. Philip Chen,[†] Dimitris Katsis,[†] and Shaw H. Chen*,[†,‡]

Contribution from the Department of Chemical Engineering and Laboratory for Laser Energetics, Center for Optoelectronics and Imaging, University of Rochester, 240 East River Road, Rochester, New York 14623-1212

Received August 4, 2003; E-mail: shch@lle.rochester.edu

Abstract: Novel nonafluorenes with a varying extent of pendant chirality were synthesized for an investigation of the origins of chiroptical activities in neat films. Thermal annealing of 4-μm-thick sandwiched films and of 90-nm-thick spin-cast films, all on surface-treated substrates, produced monodomain glassy films characterized as a right-handed cholesteric stack with a helical pitch length ranging from 180 to 534 nm and from 252 to 1151 nm, respectively. The observed strong circular dichroism (CD) and g_e as functions of helical pitch length in single-substrate monodomain glassy cholesteric films were quantitatively interpreted with a circularly polarized fluorescence theory accounting for light absorption, emission, and propagation in a cholesteric stack. Although intertwined molecular helices were likely to be present, cholesteric stacking of rodlike molecules seemed to be the predominant contributor to the strong chiroptical activities. All the cholesteric stacks comprising a polydomain glassy film on an untreated substrate were found to contribute to CD and g_e largely to the same extent as in a monodomain film. A circularly polarized blue organic light-emitting diode containing a nonafluorene film resulted in a g_e of 0.35 with a luminance yield of 0.94 cd/A at 20 mA/cm^2, the best performance to date.

Introduction

Conjugated polymers have been actively investigated since the late 1970s for their unique properties that hold enormous potential for electronic, optical, and photonic applications. Self-assemblies of conjugated polymers have also been achieved through proper derivatization for the realization of additional functionalities,[1−5] the supramolecular chirality of which is one of the most fascinating features. A major challenge today is the quantitative interpretation of strong circular dichroism (CD) and circularly polarized fluorescence (CPF) exhibited by chiral conjugated polymers in solution and neat films.[6−18] Exciton coupling theory involving chiral orientation of chromophores[14,19] and the Hartree−Fock theory for molecular helices[7] have been proposed for data interpretation. After extended thermal annealing at a temperature up to 160−200 °C, thin films of chiral poly(fluorene) and poly(*p*-phenyleneethynylene) showed liquid crystalline mesomorphism, which was suggested to account for the observed CD and CPF.[6,7,9] Moreover, computational chemistry and electron diffraction have revealed the formation of helical coils in poly(fluorene).[20] Molecular helices presented by other types of chiral conjugated polymers have also been imaged by the scanning tunneling and transmission electron microscopic techniques.[17,21] All these prior endeavors have been inconclusive as to the relative significance of exciton coupling, helical conformation, and liquid crystalline order, let alone establishing a theoretical framework for the calculation of the CD or CPF

[†] Department of Chemical Engineering.
[‡] Laboratory for Laser Energetics.

(1) Lee, M.; Cho, B.-K.; Zin, W.-C. *Chem. Rev.* **2001**, *101*, 3869−3892.
(2) Cornelissen, J. J. L. M.; Rowan, A. E.; Nolte, R. J. M.; Sommerdijk, N. A. J. M. *Chem. Rev.* **2001**, *101*, 4039−4070.
(3) Nakano, T.; Okamoto, Y. *Chem. Rev.* **2001**, *101*, 4013−4038.
(4) Mena-Osteritz, E. *Adv. Mater.* **2002**, *14*, 609−616.
(5) Kim, J.; Swager, T. M. *Nature* **2001**, *411*, 1030−1034.
(6) Oda, M.; Nothofer, H.-G.; Lieser, G.; Scherf, U.; Meskers, S. C. J.; Neher, D. *Adv. Mater.* **2000**, *12*, 362−365.
(7) Oda, M.; Nothofer, H.-G.; Scherf, U.; Šunjić, V.; Richter, D.; Regenstein, W.; Neher, D. *Macromolecules* **2002**, *35*, 6792−6798.
(8) Tang, H.-Z.; Fujiki, M.; Sato, T. *Macromolecules* **2002**, *35*, 6439−6445.
(9) Wilson, J. N.; Steffen, W.; Mckenzie, T. G.; Lieser, G.; Oda, M.; Neher, D.; Bunz, U. H. F. *J. Am. Chem. Soc.* **2002**, *124*, 6830−6831.
(10) Peeters, E.; Christiaans, M. P. T.; Janssen, R. A. J.; Schoo, H. F. M.; Dekkers, H. P. J. M.; Meijer, E. W. *J. Am. Chem. Soc.* **1997**, *119*, 9909−9910.
(11) Langeveld-Voss, B. M. W.; Janssen, R. A. J.; Christiaans, M. P. T.; Meskers, S. C. J.; Dekkers, H. P. J. M.; Meijer, E. W. *J. Am. Chem. Soc.* **1996**, *118*, 4908−4909.
(12) Meskers, S. C. J.; Peeters, E.; Langeveld-Voss, B. M. W.; Janssen, R. A. J. *Adv. Mater.* **2000**, *12*, 589−594.
(13) Langeveld-Voss, B. M. W.; Janssen, R. A. J.; Meijer, E. W. *J. Mol. Struct.* **2000**, *521*, 285−301.
(14) Catellani, M.; Luzzati, S.; Bertini, F.; Bolognesi, A. *Chem. Mater.* **2002**, *14*, 4819−4826.
(15) Goto, H.; Okamoto, Y.; Yashima, E. *Macromolecules* **2002**, *35*, 4590−4601.
(16) Zhang, Z.-B.; Fujiki, M.; Motonaga, M.; Nakashima, H.; Torimitsu, K.; Tang, H.-Z. *Macromolecules* **2002**, *35*, 941−944.
(17) Shinohara, K.-I.; Yasuda, S.; Kato, G.; Fujita, M.; Shigekawa, H. *J. Am. Chem. Soc.* **2001**, *123*, 3619−3620.
(18) Chen, H. P.; Katsis, D.; Mastrangelo, J. C.; Marshall, K. L.; Chen, S. H. *Chem. Mater.* **2000**, *12*, 2275−2281.
(19) Langeveld-Voss, B. M. W.; Beljonne, D.; Shuai, Z.; Janssen, R. A. J.; Meskers, S. C. J.; Meijer, E. W.; Brédas J.-L. *Adv. Mater.* **1998**, *10*, 1343−1348.
(20) Lieser, G.; Oda, M.; Miteva, T.; Meisel, A.; Nothofer, H.-G.; Scherf, U. *Macromolecules* **2000**, *33*, 4490−4495.
(21) Brustolin, F.; Goldoni, F.; Meijer, E. M.; Sommerdijik, N. A. J. M. *Macromolecules* **2002**, *35*, 1054−1059.

10.1021/ja037733e CCC: $25.00

Table 1. Phase Transition Temperatures of Chiral Nonafluorenes and Characteristics of Both Sandwiched and Spin-Cast Monodomain Cholesteric Films

			sandwiched film[b]				spin-cast film[f]		
compd	T_g,[a] °C	T_c,[a] °C	p_1^{SEM},[c] nm	p_1^{ell},[d] nm	λ_R,[e] nm	$\bar{n}(\lambda_R)$[d]	S[g]	p_2^{ell},[g] nm	Φ_F,[h] %
C-702	88	284	180 ± 5	na	na	na	0.77	252 ± 1	53 ± 1
C-612	91	288	272	279 ± 4	455	1.723	0.76	346 ± 6	50 ± 8
C-522	86	283	324 ± 6	325 ± 1	545	1.672	0.78	501 ± 2	59 ± 7
C-432	87	280	534 ± 9	553 ± 2	871	1.555	0.78	1151 ± 10	62 ± 4

[a] Transition temperatures gathered from DSC heating scans at 20 °C/min of samples preheated to 320 °C followed by cooling at −20 °C/min to −30 °C; T_g represents the inflection point across the glass transition and T_c the cholesteric-to-isotropic transition as identified by polarizing optical microscopy. [b] Thickness of sandwiched films defined at 4 μm by glass spacers. [c] Pitch length in sandwiched films measured with SEM. [d] Pitch length and average refractive index at λ_R in sandwiched films measured with spectroscopic ellipsometry from 450 to 1200 nm. [e] Selective reflection wavelength determined with UV−vis−near-IR spectrophotometry, not applicable to **C-702** because of excessive absorption. [f] Thickness of spin-cast films measured at 90 ± 2 nm by spectroscopic ellipsometry from 300 to 900 nm. [g] Orientational order parameter and pitch length in spin-cast films measured with spectroscopic ellipsometry from 300 to 900 nm. [h] Fluorescence quantum yield determined for annealed films.

spectra in conjugated polymer films that are highly relevant to practical application.

To overcome a general difficulty with aligning chiral conjugated polymers into monodomain liquid crystalline films (i.e., without disclinations), monodisperse oligofluorenes have been demonstrated to be promising for furnishing new insight into the origins of chiroptical activities in neat films.[22] Specifically, a nonafluorene functionalized with 2(*S*)-methylbutyl and 3(*S*),7-dimethyloctyl groups at all C-9 positions was processed into a well-aligned film on a Nylon 66 alignment layer. The resultant glassy cholesteric film was characterized as a monodomain by polarizing optical microscopy and spectroscopic ellipsometry, exhibiting dramatic CD and CPF effects. While CD was successfully interpreted on the basis of cholesteric stacking, no attempt was made to explain the CPF behavior. Furthermore, the roles played by the helical conformation and other forms of chiral assembly, which might be present in a polydomain film (i.e., with disclinations) but had not been experimentally characterized, have remained unaccounted for. The objectives of this study are (1) to synthesize a series of monodisperse chiral oligofluorenes capable of forming monodomain glassy cholesteric films with a wide range of helical pitch length, (2) to thoroughly test the predictive capability of a theory using the new materials synthesized herein, and (3) to assess the effects on CD and CPF of helical pitch length and film morphology, e.g., monodomain vs polydomain cholesteric or amorphous.

Results and Discussion

Depicted in Chart 1 are the molecular structures of monodisperse chiral nonafluorenes **C-702**, **C-612**, **C-522**, and **C-432** in which the numbers of fluorene units carrying 2(*S*)-methylbutyl, 2-methylbutyl, and 3(*S*),7-dimethyloctyl groups are designated as the first, second, and third digits, respectively. Compound **C-702** has been reported in a recent paper,[22] and the rest of the nonafluorenes were synthesized and purified following similar procedures. Further details on material synthesis and purification, validation of molecular structure by ^{1}H NMR and MALD/I-TOF MS spectra as well as elemental analysis, and the UV−vis absorption and fluorescence spectra in solution and neat films are included in the Supporting Information. As intended for this study, all nonafluorenes showed essentially identical optical spectra with an absorption

Chart 1. Molecular Structures of Chiral Nonafluorenes Synthesized for the Present Study

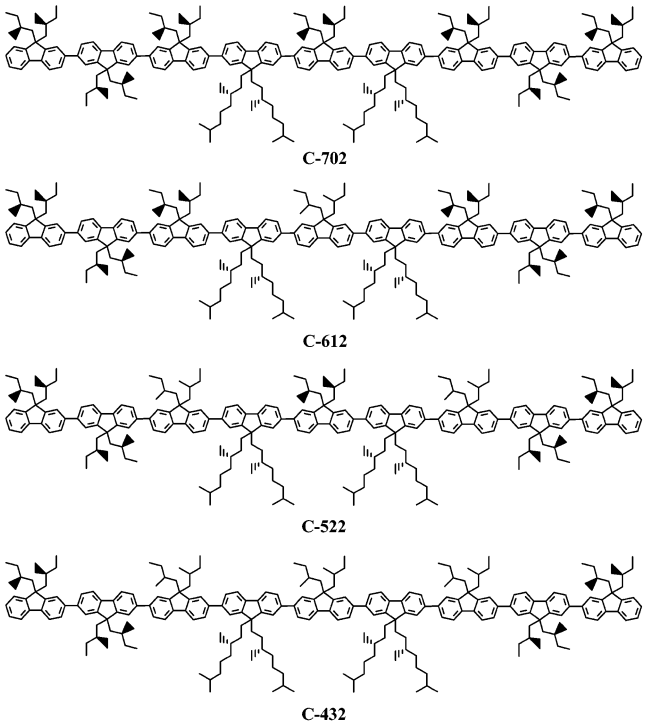

maximum at $\lambda_{max}^{ab} = 375 \pm 1$ nm and emission maxima at $\lambda_{max}^{em} = 421 \pm 1$ and 443 ± 1 nm. All four nonafluorenes were found to be thermotropic cholesteric on the basis of the oily streaks observed under hot-stage polarizing optical microscopy. To determine the thermal transition temperatures by differential scanning calorimetry (DSC), samples were preheated to 320 °C before cooling at −20 °C/min to −30 °C for gathering heating scans at 20 °C/min. The observed glass transition temperatures, T_g, and cholesteric-to-isotropic transition temperatures, T_c, are presented in Table 1. Since all nonafluorenes carry the same aliphatic pendants except chirality, little or no variation in T_g or T_c was anticipated. The absence of crystallization on heating and cooling was also noted in the DSC experiment, which is crucial to the realization of glassy cholesteric films via thermal annealing at a temperature above T_g followed by cooling to room temperature.

With the thickness defined by 4-μm glass fibers, sandwiched films were prepared by thermal processing of nonafluorene samples between two polyimide-coated and buffed fused silica

(22) Geng, Y. H.; Trajkovska, A.; Katsis, D.; Ou, J. J.; Culligan, S. W.; Chen, S. H. *J. Am. Chem. Soc.* **2002**, *124*, 8337−8347.

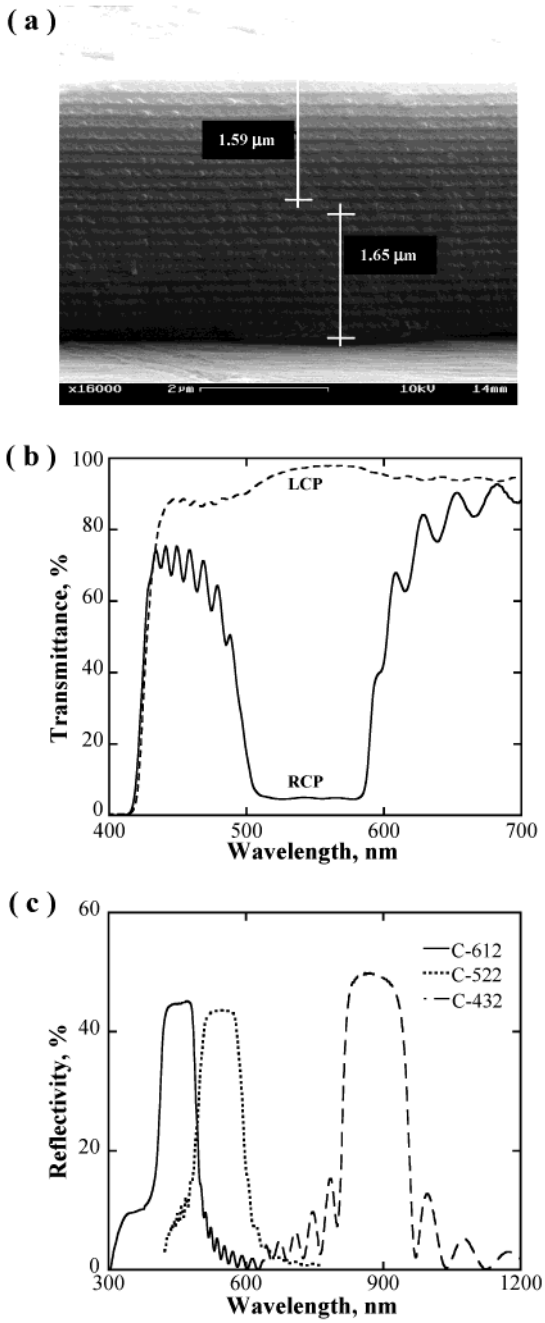

Figure 1. (a) SEM image of the cross section of a 4-μm-thick monodomain glassy cholesteric film of **C-522**. (b) Transmittances of RCP and LCP light through the same film as in (a). (c) Selective reflection spectra of 4-μm-thick monodomain glassy cholesteric films of **C-612**, **C-522**, and **C-432**.

substrates. Upon annealing and subsequent cooling to room temperature, the glassy cholesteric films in the Grandjean orientation were devoid of oily streaks under polarizing optical microscopy, viz., monodomains. As illustrated in Figure 1a, the scanning electron microscopy (SEM) image of the cross section of a **C-522** film provided a measure of the helical pitch length.[23] The p_1^{SEM} values presented in Table 1, viz., 180, 272, 324, and 534 nm for **C-702**, **C-612**, **C-522**, and **C-432**, respectively, indicate pitch loosening with a decreasing extent of pendant chirality. Furthermore, films of **C-612**, **C-522**, and **C-432** were found to consist of a right-handed cholesteric stack, as illustrated with **C-522** in Figure 1b in terms of the transmittances of right- and left-handed circularly polarized (RCP and LCP) incident light. The selective reflection spectra measured with an unpolarized incident, as shown in Figure 1c, were used to locate the selective reflection wavelength, λ_R, at the center of the reflection band. The λ_R values are reported in Table 1 except that for **C-702** because of its overwhelming light absorption in the UV region where selective reflection is expected. The annealed films were further characterized by spectroscopic ellipsometry from 450 to 1200 nm to yield $n_{||}$ and $n_{\perp}$, where the subscripts "||" and "$\perp$" denote, respectively, the directions parallel and perpendicular to the long molecular axis of nonafluorenes within quasi-nematic layers comprising the cholesteric stack. On the basis of the average refractive index, $\bar{n} = [(n_{||}^2 + 2n_{\perp}^2)/3]^{1/2}$, the helical pitch length $\lambda_R/\bar{n}$ was found to be within $\pm$3% of p_1^{SEM} from SEM imaging. As shown in Table 1, the values of the helical pitch length, p_1^{ell}, from spectroscopic ellipsometry are identical to those of p_1^{SEM} within experimental error, thus inspiring confidence in ellipsometric analysis that involves multiparameter curve fitting.

Thin films were prepared by spin coating from a 1 wt % chloroform solution on polyimide-coated and buffed fused silica substrates. Drying under vacuum produced weakly anisotropic glassy (or noncrystalline) pristine films that were annealed under argon at 20 °C above T_g for $^1/_2$ h to obtain monodomain films. These relatively thin films did not show selective reflection, unlike the 4-μm-thick films shown in Figure 1c. The monodomain character was substantiated by the angular distribution of the absorbance (at 375 nm) of a linearly polarized incident with its plane of polarization oriented along the 0−180° axis in Figure 2a. This axis is defined by the buffing direction on the alignment-coated fused silica substrate along which the first layer of nonafluorene molecules is oriented. Note that the twist angle of the axis locating maximum absorbance from the 0−180° axis is expected to increase with a decreasing p_2^{ell} for the same film thickness, as revealed in Figure 2a. The absorbance profile of a linearly polarized incident was predicted for a monodomain cholesteric film. On the basis of the Jones matrix, a numerical method was developed for the treatment of multiple reflections in a cholesteric film,[24] to which light absorption was added in this study. The computer program with a summary of underlying equations is furnished as part of the Supporting Information. It is demonstrated in Figure 2a that the experimental data follow closely the calculation in solid curves with input information from ellipsometric analysis without resorting to adjustable parameters.

Modeled as a monodomain cholesteric stack with a constant pitch length, p_2^{ell}, the annealed spin-cast films were characterized by spectroscopic ellipsometry from 300 to 900 nm to furnish the film thickness, the anisotropic absorption coefficients, $\alpha_{||}$ and $\alpha_{\perp}$, p_2^{ell}, $n_{||}$ and $n_{\perp}$, and the helical sense. All four annealed films were found to comprise a right-handed cholesteric stack with the same film thickness, 90 $\pm$ 2 nm, and nearly identical anisotropic absorption and refractive index profiles, as shown for **C-702** in Figure 3a in which $\bar{n}(\lambda)$ is also included. With $\alpha_{||}$ and $\alpha_{\perp}$ at 375 nm from the spectra shown in Figure 3b, the orientational order parameter governing nonafluorene molecules within quasi-nematic layers was calculated according

(23) Bunning, T. J.; Vezie, D. L.; Lloyd, P. F.; Haaland, P. D.; Thomas, E. L.; Adams, W. W. *Liq. Cryst.* **1994**, *16*, 769−781.

(24) Yang, D.-K.; Mi, X.-D. *J. Phys. D: Appl. Phys.* **2000**, *33*, 672−676.

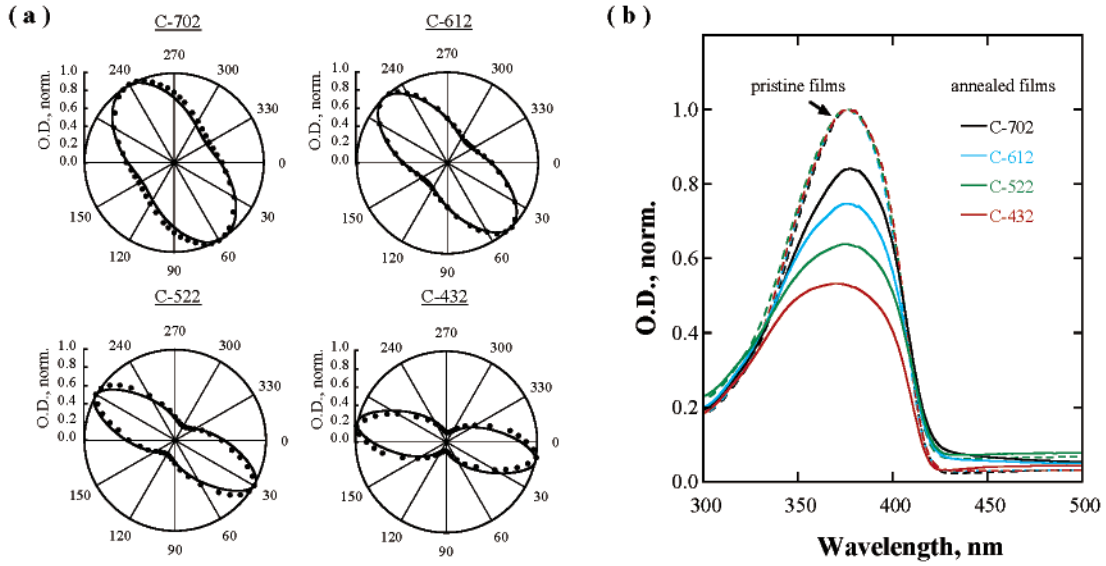

Figure 2. (a) Angular distribution of absorbance at 375 nm of a linearly polarized incident, with its plane of polarization oriented along the 0−180° axis, through 90-nm-thick monodomain glassy cholesteric films of **C-702**, **C-612**, **C-522**, and **C-432**. (b) Hypochromism as demonstrated by a comparison of the UV−vis absorption spectra of weakly anisotropic pristine films with those of monodomain glassy cholesteric films of **C-702**, **C-612**, **C-522**, and **C-432**, all with a thickness of 90 ± 2 nm.

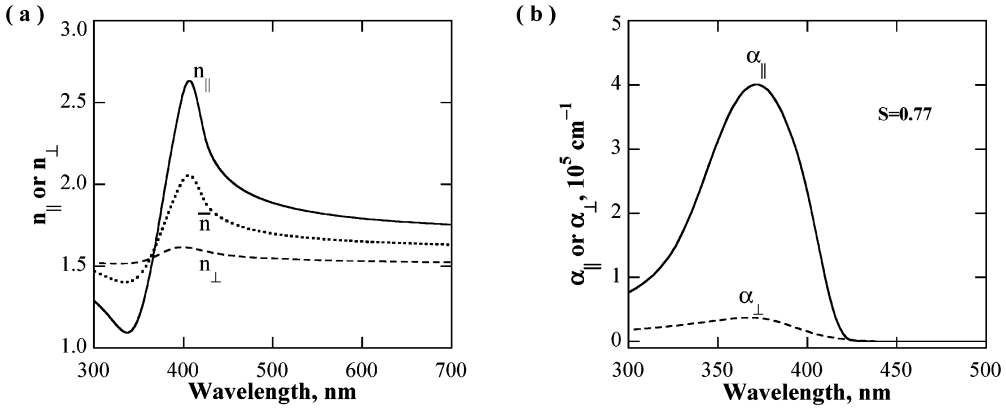

Figure 3. Ellipsometric analysis of a 90-nm-thick monodomain glassy cholesteric film of **C-702**: (a) refractive index parallel, $n_{\|}$, and that perpendicular, $n_{\perp}$, to the long molecular axis within quasi-nematic layers comprising a cholesteric stack, and the average refractive index characterizing the quasi-nematic layers, $\bar{n} = [(n_{\|}^2 + 2n_{\perp}^2)/3]^{1/2}$; (b) absorption coefficient parallel, $\alpha_{\|}$, and that perpendicular, $\alpha_{\perp}$, to the long molecular axis within quasi-nematic layers.

to $S = (R - 1)/(R + 2)$, in which the dichroic ratio, R, is equal to $\alpha_{\|}/\alpha_{\perp}$. An S value of 0.77 ± 0.01 listed in Table 1 is indicative of a high degree of uniaxial molecular alignment. As also shown in Table 1, p_2^{ell} is consistently longer than p_1^{ell} because of the stronger surface anchoring in 90-nm-thick spin-cast films than in 4-μm-thick sandwiched films. In both cases, the helical pitch length increases with a decreasing extent of pendant chirality. At an increasing p_2^{ell}, the twist angle decreases between nonafluorene molecules in adjacent quasi-nematic layers, thus allowing for an increasing overlap between molecular orbitals manifested as a more pronounced hypochromism as shown in Figure 2b, where absorbances of annealed films are compared to those of pristine films. However, the fluorescence quantum yield, Φ_F, of ≅55% was obtained in all cases according to Table 1, indicating its independence on the twist angle between neighboring oligofluorene molecules.

To gain fundamental insight into the origins of chiroptical activities in thin films, CPF was characterized with unpolarized excitation at 370 nm in terms of $g_e \equiv 2(I_L - I_R)/(I_L + I_R)$, where I_L and I_R represent the left- and right-handed circularly polarized emission intensities, respectively. As shown in Figure 4a, a negative g_e resulted from pristine films on a buffed polyimide alignment layer. A similar observation was made for a **C-702** film on a buffed Nylon 66 alignment layer, which was attributed to left-handed intertwined molecular helices on the basis of molecular mechanics simulation.[22] Upon thermal annealing into a right-handed cholesteric stack as dictated by the energetics governing molecular packing,[25] a positive g_e emerged, as presented in Figure 4b for the four nonafluorenes. It is evident that cholesteric stacking plays a predominant role over the helical molecular conformation in the g_e profiles of the annealed films. The fact that rodlike poly(*p*-phenylene)s with chiral pendants formed cholesteric stacking[18,26] suggests that the helical conformation is not a necessary condition for cholesteric stacking in general. Good and Karali[27] constructed a theory for circular polarization of incident light as a result of light propagation through a cholesteric stack using the real part of

(25) Sato, T.; Sato, Y.; Umemura, Y.; Teramoto, A.; Nagamura, Y.; Wagner, J.; Weng, D.; Okamoto, Y.; Hatada, K.; Green, M. M. *Macromolecules* **1993**, *26*, 4551−4559.
(26) Katsis, D.; Chen, H. P.; Chen, S. H.; Rothberg, L. J.; Tsutsui, T. *Appl. Phys. Lett.* **2000**, *77*, 2982−2984.
(27) Good, R. H., Jr.; Karali, A. *J. Opt. Soc. Am. A* **1994**, *11*, 2145−2155.

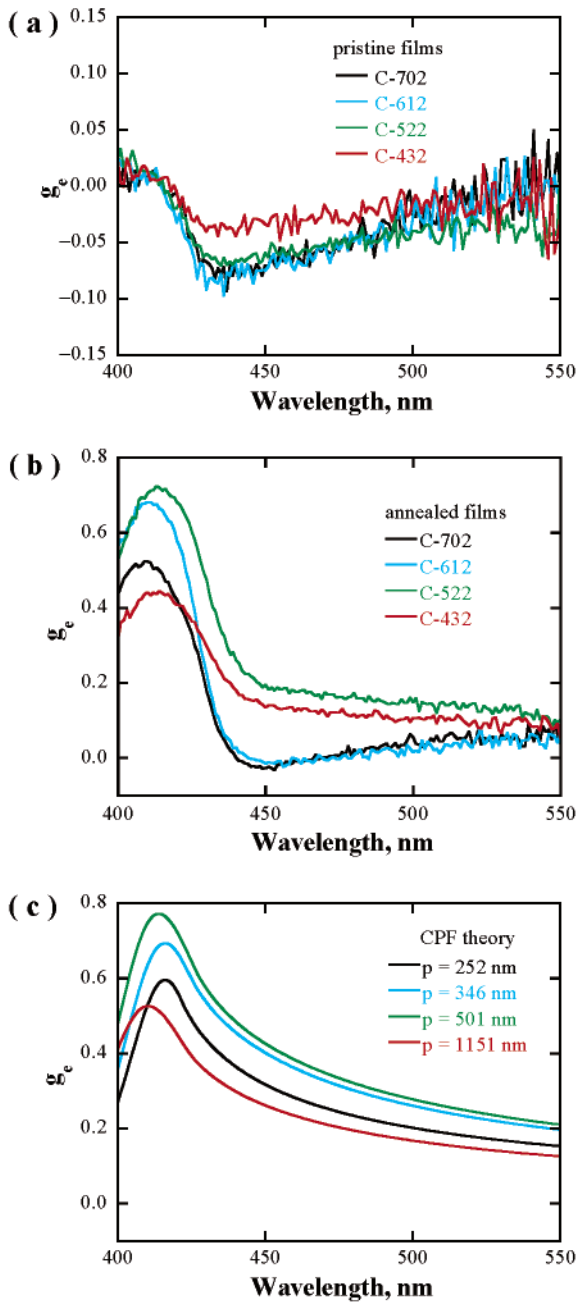

Figure 4. g_e profiles of 90-nm-thick spin-cast films on a surface-treated substrate of **C-702**, **C-612**, **C-522**, and **C-432**: (a) weakly anisotropic pristine glassy films after vacuum drying; (b) monodomain glassy cholesteric films after thermal annealing; (c) prediction by a CPF theory.

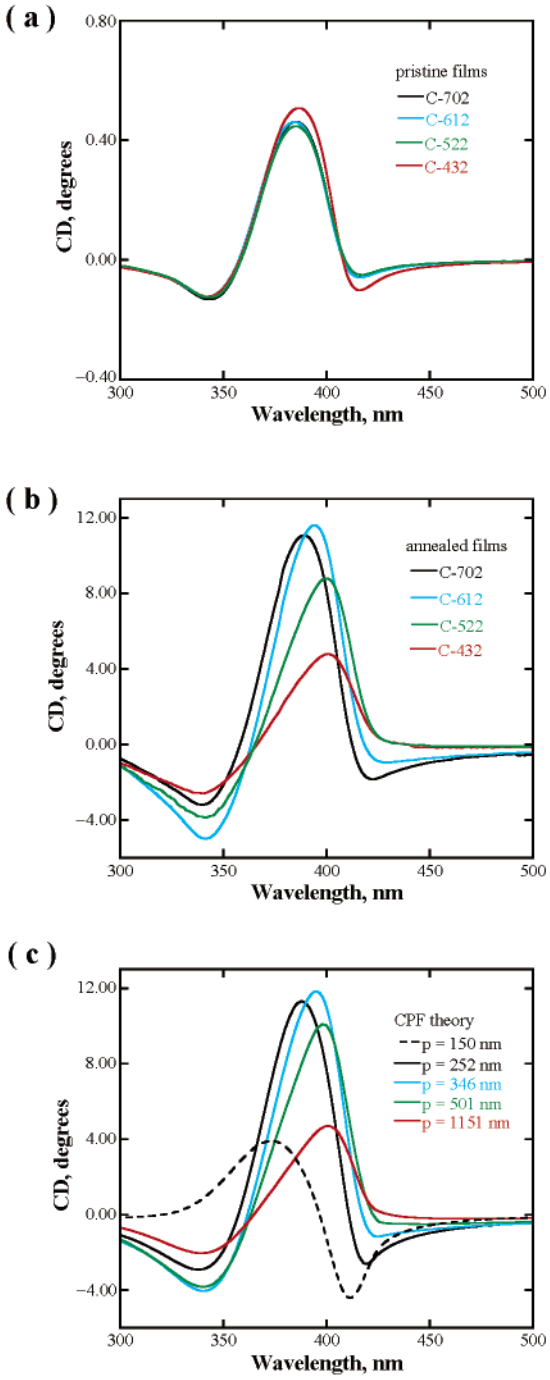

Figure 5. CD spectra of 90-nm-thick spin-cast films on a surface-treated substrate of **C-702**, **C-612**, **C-522**, and **C-432**: (a) weakly anisotropic pristine glassy films after vacuum drying; (b) monodomain glassy cholesteric films after thermal annealing; (c) prediction by CPF theory for the four nonafluorenes plus a hypothetical system with a helical pitch length of 150 nm.

the dielectric constant. Shi et al.[28] generalized the Good−Karali theory for circularly polarized fluorescence with simultaneous circular dichroism and circular polarization of propagating excitation and emission light through the film by incorporation of a complex dielectric constant. In essence, the CPF theory describes CD and CPF of rigid rods placed in a cholesteric stack. It was experimentally validated for emission outside the resonance region, viz., the selective reflection band of a micrometer-thick film where multiple reflections occur.[28] Without accounting for multiple reflections in micrometer-thick films, the CPF theory failed to explain the dramatic variation in g_e for light emission in the resonance region.[29] In the absence of a resonance region in films less than 100 nm thick, as encountered in this study, the CPF theory should be applicable anywhere in the optical spectrum. With all the model parameters independently determined by spectroscopic ellipsometry, including wavelength dispersion of refractive indices, the g_e profiles predicted by the CPF theory are presented in Figure 4c for

(28) Shi, H.; Conger, B. M.; Katsis, D.; Chen, S. H. *Liq. Cryst.* **1998**, *24*, 163−172.

(29) Chen, S. H.; Katsis, D.; Schmid, A. W.; Mastrangelo, J. C.; Tsutsui, T.; Blanton, T. N. *Nature* **1999**, *397*, 506−508.

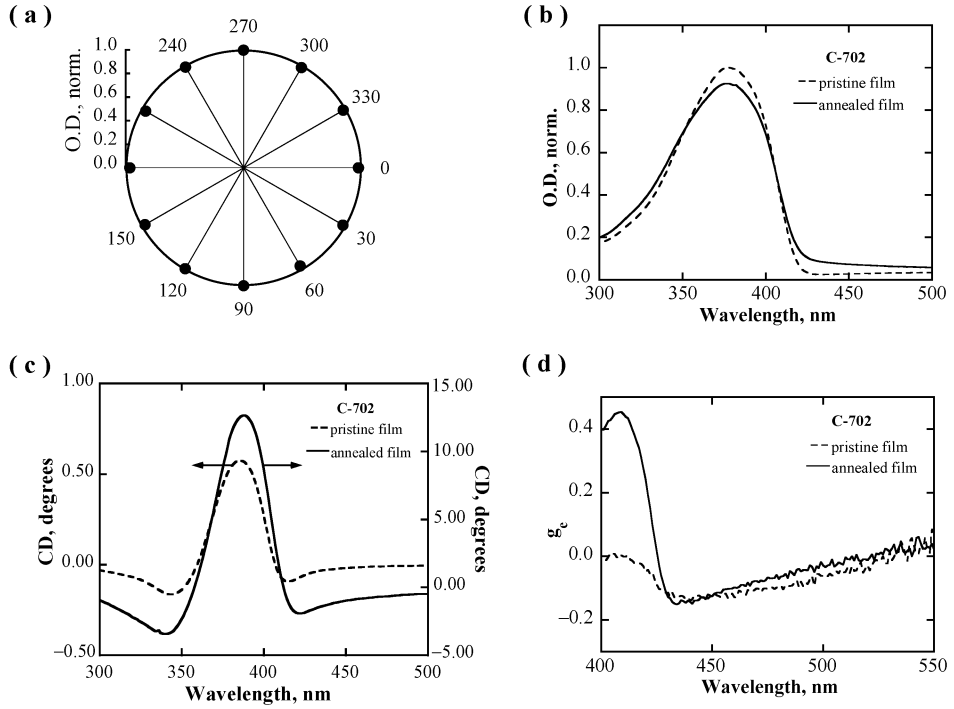

Figure 6. A 90-nm-thick spin-cast film of **C-702** on an untreated substrate: (a) characteristics of a polydomain glassy cholesteric film, after thermal annealing, as demonstrated by the angular distribution of absorbance at 375 nm of a linearly polarized incident; (b) absorption spectrum of a pristine film compared to that of an annealed film, revealing a lesser extent of hypochromism than that in the monodomain film shown in Figure 2b; (c) CD spectrum of a pristine film compared to that of an annealed film; (d) g_e profile of a pristine film compared to that of an annealed film.

helical pitch lengths of 252, 346, 501, and 1151 nm corresponding to the four nonafluorenes. It appears that the experimental observation of g_e for the annealed films represents approximately the sum of the theoretical prediction for a cholesteric stack and the experimental observation of pristine films. Therefore, one may surmise that the annealed monodomain film consists of a right-handed cholesteric stack of intertwined molecular helices.

As shown in Figure 5a, the maximum CD values of all pristine films are about 0.5°. An order-of-magnitude enhancement in CD resulted from thermal annealing into a right-handed cholesteric stack, as Figure 5b is compared to Figure 5a. To further substantiate the existence of a cholesteric stack, the CPF theory was tested with $\alpha_{\parallel}$ and $\alpha_{\perp}$, $n_{\parallel}$ and $n_{\perp}$, the film thickness, and the helical sense and pitch length independently determined by spectroscopic ellipsometry as described above. As demonstrated in Figure 5c versus Figure 5b, the agreement between theory and experiment is remarkable, further supporting the view that thermally annealed films consist of a cholesteric stack of nonafluorene molecules, resulting in the strong chiroptical activities. It is no surprise that the CPF theory delineates CD to a better accuracy than g_e mainly because the optical parameters as input information to the theory were determined through ellipsometry involving absorption but no emission measurements. With confidence in the CPF theory, the CD spectrum was predicted for a helical pitch length of 150 nm in a 90-nm-thick film; see the dashed curve in Figure 5c. Note the bisignate CD spectrum originating from a tightly pitched cholesteric stack without considering exciton coupling within the framework of the CPF theory as pursued in this study.

To unravel the effect of an alignment layer on chiroptical properties, a film of **C-702** was prepared on an untreated fused silica substrate by spin coating under the same conditions as that on a surface-treated substrate. The vacuum-dried films on these two types of substrates were found to possess the same thickness, 90 nm, on the basis of absorbance at 375 nm. Thermal annealing turned an optically isotropic pristine film into a polydomain glassy film in view of the Schlieren textures observed under polarizing optical microscopy as expected of a thin cholesteric film. Because of the polydomain morphology, ellipsometric analysis failed to model the annealed film as a single cholesteric stack (i.e., a monodomain film). A polydomain film comprises many cholesteric stacks in the Grandjean orientation, each having its own set of rotating molecular axes characterizing quasi-nematic layers while all completing the same degree of helical twisting across the film thickness. The polydomain character was substantiated in Figure 6a by the expected uniform absorbance profile of a linearly polarized incident for the same thickness as that of monodomain films shown in Figure 2a. Thermal annealing resulted in hypochromism, as shown in Figure 6b, albeit to a lesser extent than in the monodomain film on a surface-treated substrate shown in Figure 2b. The pristine film on an untreated substrate yielded CD and g_e profiles close to those on a surface-treated substrate, as parts c and d of Figure 6 are compared to Figures 5a and 4a, respectively. Similarly, the CD and g_e profiles of the annealed polydomain film on an untreated substrate are comparable to those of the annealed monodomain film on a buffed polyimide alignment layer. It is thus concluded that whether a film is monodomain is not critical to chiroptical activities because all the cholesteric stacks comprising a polydomain film contribute equally, and in the same way as a monodomain film as a whole, to the observed CD and g_e.

For the fabrication of a circularly polarized blue organic light-emitting diode (OLED), **C-522** was selected for its g_e superior to those of the other nonafluorenes, as shown in Figure 3b. A

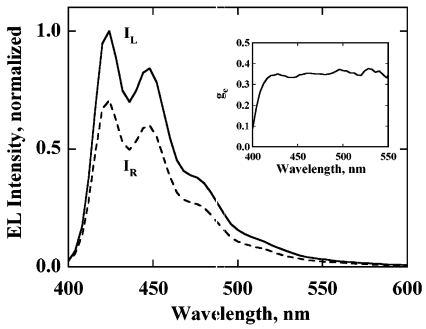

Figure 7. Circularly polarized electroluminescence spectra of an OLED device containing a 70-nm-thick monodomain glassy cholesteric film of **C-522** with an inset displaying the resultant g_e profile.

C-522 film was prepared by spin coating from a 0.8 wt % chloroform solution as part of the device structure ITO(35 nm)/PEDOT:PSS(40 nm)/C-522(70 nm)/TPBI(30 nm)/LiF(0.5 nm)/Mg:Ag(20:1;210 nm), where poly(3,4-ethylenedioxythiophene)/poly(styrenesulfonic acid), PEDOT/PSS, serves as the buffed alignment layer, instead of polyimide, to facilitate hole injection and transport.[30] A turn-on voltage of less than 5V was observed. At a current density of 20 mA/cm^2, this device showed a luminance yield of 0.94 cd/A and Commission Internationale de l'Eclairage (CIE) coordinates of (0.157, 0.068), both measured without polarization analysis. The CIE coordinates indicate that the device prepared with **C-522** emits light closer to the standard blue than those previously reported using poly(fluorene)s.[6] The circularly polarized electroluminescence spectra are presented in Figure 7, which were used to calculate g_e as defined above. The g_e profile included as an inset indicates a value of 0.35, which is higher than any of the previously reported values for conjugated polymers.[6,10] The relatively constant g_e value across most of the emission spectrum suggests a narrow recombination zone near the interface with the electron transport layer, thus enabling all emitted light to be processed to the same extent.

Conclusions

Novel nonafluorenes were synthesized with pendant chirality modulated by the relative abundance of 2(*S*)-methylbutyl, 2-methylbutyl, and 3(*S*),7-dimethyloctyl groups at the C-9 positions of all fluorene units. Neat films were prepared by melt processing and spin coating for characterization by polarizing optical microscopy, scanning electron microscopy, UV−vis−near-IR spectrophotometry, spectroscopic ellipsometry, circular dichroism, circularly polarized fluorescence, and electroluminescence. Key observations are summarized as follows.

(1) Thermal annealing of 4-μm-thick sandwiched films between surface-treated fused silica substrates resulted in monodomain glassy films comprising a right-handed cholesteric stack in the Grandjean orientation with a helical pitch length ranging from 180 to 534 nm determined by SEM and spectroscopic ellipsometry. The selective reflection wavelength was characterized by UV−vis−near-IR spectrophotometry to vary from less than 400 to 871 nm, consistent with the independently measured helical pitch length and average refractive index.

(2) Pristine films, 90 nm in thickness, on a surface-treated substrate were weakly anisotropic, and hence not amenable to ellipsometric analysis. Thermal annealing produced monodomain glassy films, as corroborated by polarized UV−vis spectrophotometry. The monodomain films were characterized by ellipsometry to consist of a right-handed cholesteric stack in the Grandjean orientation with a helical pitch length ranging from 252 to 1151 nm. The longer pitch length in a spin-cast film than in a sandwiched film was attributed to the stronger surface anchoring in a thinner film.

(3) At a thickness of 90 nm, the annealed films on a surface-treated substrate showed a CD up to 12°, an enhancement by a factor of 20 over that of pristine films. Annealed and pristine films exhibited absolute values of g_e up to 0.72 and 0.08, respectively. The results from the annealed films were quantitatively interpreted with a CPF theory for a cholesteric stack across a wide range of helical pitch length. Although intertwined molecular helices were likely to be present, cholesteric stacking of rodlike molecules seemed to be the predominant contributor to the observed CD and g_e.

(4) A 90-nm-thick annealed film of **C-702** on an untreated substrate was found to be a polydomain, as revealed by polarized UV−vis spectrophotometry, and hence could not be analyzed by ellipsometry. However, the polydomain glassy cholesteric film showed a CD and g_e both comparable to those of a monodomain film of **C-702**, an observation attributable to the fact that all the cholesteric stacks comprising a polydomain film contribute equally, and in the same way as the monodomain film, to the observed chiroptical activities.

(5) A 70-nm-thick monodomain glassy cholesteric film of **C-522** was integrated into a blue OLED, showing a turn-on voltage of less than 5 V, a luminance yield of 0.94 cd/A, a g_e value of 0.35, and CIE coordinates of (0.157, 0.068), all at a current density of 20 mA/cm^2, representing the best performing circularly polarized OLED to date.

Acknowledgment. We thank C. W. Tang, K. M. Vaeth, and K. Klubek for their contributions to the fabrication and characterization of a circularly polarized OLED and A. J. Hoteling for the MALD/I-TOF measurement and analysis, all at Eastman Kodak Co. in Rochester, NY. We also thank S. D. Jacobs and K. L. Marshall at the University of Rochester for helpful discussions regarding material characterization. We are grateful for the financial support provided by the National Science Foundation under Grant CTS-0204827 and the Multidisciplinary University Research Initiative, administered by the Army Research Office, under Grant DAAD19-01-1-0676. Additional funding was provided by the Department of Energy Office of Inertial Confinement Fusion under Cooperative Agreement No. DE-FC03-92SF19460 with the Laboratory for Laser Energetics and the New York State Energy Research and Development Authority.

Supporting Information Available: Synthesis and purification procedures with ^{1}H NMR spectral data for all the intermediates and final products, UV−vis absorption spectra in dilute solution, UV−vis absorption and circularly polarized fluorescence spectra in neat films, and computer program for the distribution of absorbance of linearly polarized incident light through a cholesteric stack with a summary of equations (PDF). This material is available free of charge via the Internet at http://pubs.acs.org.

JA037733E

(30) Culligan, S. W.; Geng, Y. H.; Chen, S. H.; Klubek, K.; Vaeth, K. M.; Tang, C. W. *Adv. Mater.* **2003**, *15*, 1176−1180.